

# Chemical Equilibrium in Collisions of Small Systems

I. Kraus<sup>1,2</sup>, J. Cleymans<sup>1,3,4</sup>, H. Oeschler<sup>1</sup>, K. Redlich<sup>4,5</sup> and S. Wheaton<sup>1,3</sup>

<sup>1</sup>*Institut für Kernphysik, Darmstadt University of Technology, D-64289 Darmstadt, Germany*

<sup>2</sup>*Nikhef, Kruislaan 409, 1098 SJ Amsterdam, The Netherlands*

<sup>3</sup>*UCT-CERN Research Centre and Department of Physics,  
University of Cape Town, Rondebosch 7701, South Africa*

<sup>4</sup>*Universität Bielefeld, Fakultät für Physik, D-33615 Bielefeld, Germany*

<sup>5</sup>*Institute of Theoretical Physics, University of Wrocław, PL-45204 Wrocław, Poland*

(Dated: February 1, 2008)

The system-size dependence of particle production in heavy-ion collisions at the top SPS energy is analyzed in terms of the statistical model. A systematic comparison is made of two suppression mechanisms that quantify strange particle yields in ultra-relativistic heavy-ion collisions: the canonical model with strangeness correlation radius determined from the data and the model formulated in the canonical ensemble using chemical off-equilibrium strangeness suppression factor. The system-size dependence of the correlation radius and the thermal parameters are obtained for p-p, C-C, Si-Si and Pb-Pb collisions at  $\sqrt{s_{NN}} = 17.3$  AGeV. It is shown that on the basis of a consistent set of data there is no clear difference between the two suppression patterns. In the present study the strangeness correlation radius was found to exhibit a rather weak dependence on the system size.

PACS numbers: 25.75.-q, 25.75.Dw

Keywords: Statistical model, Strangeness undersaturation, Relativistic heavy-ion collisions, Particle production

## I. INTRODUCTION

Experiments with ultra-relativistic nucleus-nucleus collisions provide a unique opportunity to study the properties of strongly interacting matter under the extreme condition of high energy densities. Hadronic multiplicities, and their spectra in particular, carry information about the nature of the medium from which they originated. The statistical model (SM) has been recognized as a powerful approach to describe particle production yields in heavy-ion collisions [1, 2]. These models assume that particle creation occurs at chemical freeze-out with the collision fireball being in thermal and chemical equilibrium.

In the limit of high temperature and/or large system size, the grand-canonical (GC) treatment of strangeness conservation is adequate in the SM. There, strangeness conservation is implemented on the average and is controlled by the chemical potential [1, 2]. However, if the number of strange particles in a collision fireball is small, either due to low temperature (e.g. in A-A collisions at incident energies of a few AGeV [3]) or due to small system size (e.g. in a fireball created in p-p or light-ion collisions), then strangeness conservation has to be implemented exactly in the canonical (C) ensemble [1, 4, 5, 6, 7, 8, 9]. Exact strangeness conservation leads to the suppression of the strange particle's phase-space and is usually referred to as canonical suppression [4, 6, 7]. However, canonical suppression with the assumption of strangeness chemical equilibrium in the whole fireball volume was found to be insufficient to reproduce the observed yields in nucleus-nucleus collisions at the SPS [3, 9, 10, 11, 12]. In this paper we consider a method to account for the suppression beyond

the one expected in the canonical ensemble by assuming that exact strangeness conservation holds only in a small sub-volume  $V_C$  of the system [1, 4, 7]. The concept of such a sub-volume, or a strangeness correlation volume, has been used in earlier studies [5, 13, 14, 15]. Here, we present a systematic analysis of p-p and central C-C, Si-Si and Pb-Pb collisions at the top SPS energy from the NA49 collaboration [16, 17, 18, 19, 20, 21, 22, 23, 24]. We selected a consistent set of data (discussed below) for different collision systems and focus only on central nucleus-nucleus collisions. We test the validity of the above approach and study the relation between  $V_C$  and the system size, and also the chemical freeze-out volume. The results of the canonical model with cluster formation will be compared to those obtained in the canonical model with strangeness suppression through chemical off-equilibrium factor  $\gamma_S$ .

The paper is organized as follows: A short outline of the statistical model and its canonical formulation with cluster formation is given in Section II. In Section III, the data analysis is presented followed by a comparison of the models with the data in Section IV. The paper concludes in Section V with a discussion.

## II. THE MODEL DESCRIPTION

### A. Grand-canonical ensemble

In the statistical model the thermal fireball is characterized by its volume  $V$ , temperature  $T$  and charge chemical potentials  $\bar{\mu}$  which are assumed to be uniform over the whole volume. In the GC ensemble, these parameters determine the partition function  $Z(T, V, \bar{\mu})$ . In

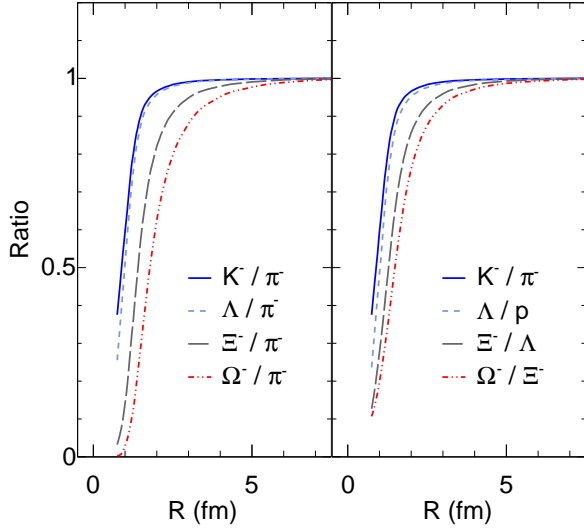


FIG. 1: Different particle ratios as a function of the radius  $R$  of a spherical volume. The temperature  $T = 170$  MeV and the baryon chemical potential  $\mu_B = 255$  MeV were chosen according to the thermal conditions at top SPS energy. All ratios are normalized to their grand-canonical values.

the hadronic fireball of non-interacting particles and resonances,  $\ln Z$  is the sum of the contributions of all  $i$ -particle species of energy  $E_i$  and spin-isospin degeneracy  $g_i$  by,

$$\frac{1}{V} \ln Z(T, V, \vec{\mu}) = \sum_i Z_i^1(T, \vec{\mu}), \quad (1)$$

with,

$$Z_i^1 = \pm \frac{g_i}{2\pi^2} \int_0^\infty p^2 dp \ln \left[ 1 \pm \exp\left(\frac{\vec{q}_i \vec{\mu} - E_i}{T}\right) \right], \quad (2)$$

where  $\vec{q}_i = (B_i, S_i, Q_i)$  are the quantum numbers of particle  $i$  and  $\vec{\mu} = (\mu_B, \mu_S, \mu_Q)$  are the chemical potentials related to the conservation of baryon number, strangeness and electric charge, respectively. The upper (lower) signs refer to fermions (bosons).

In a fireball created in heavy-ion collisions only the baryon chemical potential  $\mu_B$  is an independent parameter while the other two, the charge  $\mu_Q$  and the strangeness  $\mu_S$  chemical potentials, are constrained by the initial conditions from the electric charge of the incoming nuclei and the condition of strangeness neutrality.

The partition function (1) contains all information to obtain the number density  $n_i$  of thermal particle species  $i$ . Introducing the particle's specific chemical potential  $\mu_i$ , one gets,

$$n_i(T, \vec{\mu}) = \frac{1}{V} \frac{\partial(T \ln Z)}{\partial \mu_i} \Big|_{\mu_i=0}. \quad (3)$$

The thermally produced resonances that decay into species  $i$  contribute to the measured yield. Therefore, the contributions from all heavier particles  $j$  that decay

to hadron  $i$  with the branching fraction  $\Gamma_{j \rightarrow i}$  have to be calculated as,

$$n_i^{decay} = \sum_j \Gamma_{j \rightarrow i} n_j. \quad (4)$$

Consequently, the final yield  $N_i$  of particle species  $i$  is the sum of the thermally produced particles and the decay products of resonances,

$$N_i = (n_i + n_i^{decay}) V. \quad (5)$$

From Eqs. (3-5) it is clear that in the GC ensemble the particle yields are determined by the volume of the fireball, its temperature and the baryon chemical potential.

## B. Canonical ensemble

In general, if the number of particles carrying quantum numbers related to a conservation law is small, then the grand-canonical description no longer holds. In such a case conservation of charges has to be implemented exactly in the canonical ensemble. Here, we refer only to strangeness conservation and consider charge and baryon number conservation to be fulfilled on the average in the GC ensemble because the number of charged particles and baryons is much larger than that of strange particles. The density of strange particle  $i$  carrying strangeness  $s$  can be obtained in the canonical ensemble from,

$$n_i^C = \frac{Z_i^1}{Z_{S=0}^C} \sum_{k=-\infty}^{\infty} \sum_{p=-\infty}^{\infty} a_3^p a_2^k a_1^{-2k-3p-s} I_k(x_2) I_p(x_3) I_{-2k-3p-s}(x_1), \quad (6)$$

where  $Z_{S=0}^C$  is the canonical partition function

$$Z_{S=0}^C = e^{S_0} \sum_{k=-\infty}^{\infty} \sum_{p=-\infty}^{\infty} a_3^p a_2^k a_1^{-2k-3p} I_k(x_2) I_p(x_3) I_{-2k-3p}(x_1), \quad (7)$$

and  $Z_i^1$  is the one-particle partition function (2) calculated for  $\mu_S = 0$  in the Boltzmann approximation. The arguments of the Bessel functions  $I_s(x)$  and the parameters  $a_i$  are introduced as,

$$a_s = \sqrt{S_s/S_{-s}}, \quad x_s = 2V \sqrt{S_s S_{-s}}, \quad (8)$$

where  $S_s$  is the sum of all  $Z_k^1(\mu_S = 0)$  from (2) for particle species  $k$  carrying strangeness  $s$ .

In the limit where  $x_n < 1$  (for  $n = 1, 2$  and  $3$ ) the density of strange particles (6) carrying strangeness  $s$  is well approximated by [1],

$$n_i^C \simeq n_i \frac{I_s(x_1)}{I_0(x_1)}. \quad (9)$$

From this equation it is clear that in the C ensemble the strange particle density depends explicitly on the volume  $V$  through the arguments of the Bessel functions. In addition, as seen in Eq. (9), the strange particle densities are suppressed in the C ensemble due to exact strangeness conservation constraints.

The canonical suppression relative to the GC results for different particle ratios is illustrated in Fig. 1 for fixed  $T$  and  $\mu_B$  and for different system sizes parameterized by the radius  $R$ , assuming spherical geometry of the volume  $V$ . The left-hand panel illustrates that the canonical suppression increases with the strangeness content of the particle [1]. For  $R > 5$  fm the canonical suppression is already so small that the C and GC descriptions of particle ratios are equivalent. The right-hand panel shows the particle ratios with a difference in their strangeness quantum numbers,  $\Delta S = 1$ . Interestingly, the canonical suppression of these ratios is similar but not identical. Thus, the C-suppression in these ratios depends on the strangeness content of both hadrons and not only on the difference.

### C. Strangeness suppression mechanisms

In the application of the statistical model to particle production in heavy-ion and particularly in elementary particle collisions it was found that canonical suppression alone is not sufficient to quantify the observed strange particle yields [6]. Consequently, additional suppression mechanisms were proposed to account for deviations from experimental data. Here we present two methods that lead to additional suppression of strange particle phase-space going beyond the normal canonical effect [1, 5, 7].

The suppression of strangeness has been parameterized by a factor,  $\gamma_S$ , that is introduced to suppress hadrons composed of strange and/or anti-strange quarks [10]. In this description the strange particle density (3) composed of  $s$  strange quarks/antiquarks is modified in the GC ensemble by,

$$n_i \rightarrow \gamma_S^s n_i, \quad (10)$$

where  $\gamma_S$  is an additional parameter of the model. This chemical off-equilibrium factor also modifies the calculation of the canonical suppression outlined in Eqs. (6-8), the single-particle partition function  $Z_k^1$  is replaced by  $\gamma_S^s Z_k^1$ .

In order to account for an additional strangeness suppression in terms of the canonical model we use the concept of strangeness correlation in clusters of sub-volume  $V_C \leq V$  [1]. Consequently, there are two volume parameters in the model; the overall volume of the system  $V$ , which determines the particle yields at fixed density and the strangeness correlation (cluster) volume  $V_C$ , which enters through the canonical suppression factor and reduces the densities of strange particles. Hence, this results in replacing the volume  $V$  by  $V_C$  in Eq. (8). Assuming spherical geometry, the volume  $V_C$  is parameter-

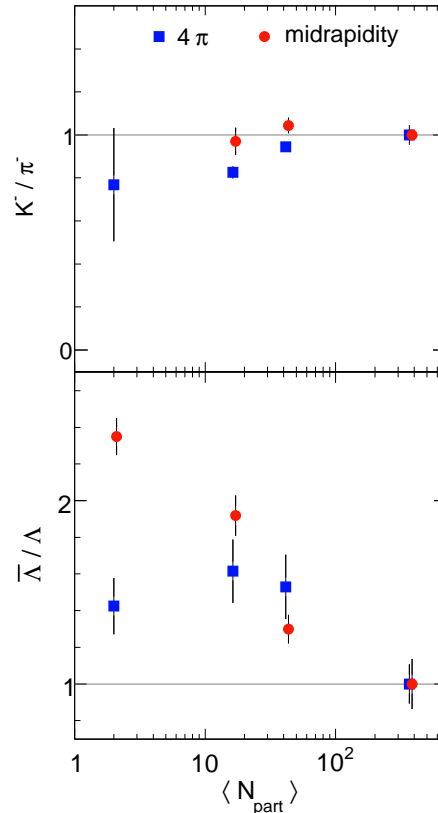


FIG. 2: Midrapidity (circles) and  $4\pi$  (squares) data on the  $\bar{\Lambda}/\Lambda$  and  $K^-/\pi^-$  ratios in p-p and central C-C, Si-Si and Pb-Pb collisions normalized to the Pb-Pb measurement [16, 17, 19, 20, 21, 22].

ized by the radius  $R_C$  which serves as a free parameter and defines the range of local strangeness equilibrium. A particle with strangeness quantum number  $s$  can appear anywhere in the volume  $V$ . However, it has to be accompanied within the sub-volume  $V_C$  by other particles carrying strangeness  $-s$  to conserve strangeness exactly.

In the application of the SM to particle production and their system-size dependence we consider three different formulations of the model:

- (a) equilibrium model in the canonical ensemble with strangeness correlation volume  $V_C = V$ ,
- (b) non-equilibrium canonical model with strangeness undersaturation parameterized by the factor  $\gamma_S$ ,
- (c) canonical model that accounts for strangeness correlation in the sub-volume  $V_C \leq V$  that is quantified by the cluster radius  $R_C$ .

In the following we compare the above models with experimental data at the top SPS energy for different colliding systems. We focus on the system-size dependence

TABLE I: Particle yields ( $4\pi$  integrated) in minimum bias p-p collisions at  $\sqrt{s_{NN}} = 17.3$  GeV from Ref. [17, 19] and fit results from model (c).

Particle	p-p	
	Data	Fit
$\pi^+/\pi^-$	$1.23 \pm 0.26$	1.23
$K^+/K^-$	$1.61 \pm 0.61$	1.65
$\bar{\Lambda}/\Lambda$	$0.118 \pm 0.013$	0.118
$K^-/\pi^-$	$0.062 \pm 0.021$	0.062
$\Lambda/K^+$	$0.450 \pm 0.138$	0.441
$\bar{\Lambda}/K^-$	$0.085 \pm 0.027$	0.086
$\pi^-$	$2.57 \pm 0.36$	2.57

of the thermal parameters with particular emphasis on the change in the strangeness correlation radius  $R_C$ .

### III. DATA SETS

To verify the statistical nature of particle production in heavy-ion collisions for different colliding systems we consider the experimental data at the top SPS energy with  $\sqrt{s_{NN}} = 17.3$  AGeV, from p-p and central C-C, Si-Si and Pb-Pb collisions [16, 17, 18, 19, 20, 21, 22, 23, 24]. In view of the fact that only a limited number of hadrons were experimentally analyzed in the smaller systems, we restrict our study to a consistent set of data [16, 17, 19, 21, 22]. Therefore, e.g. the multi-strange particles are not included as they are not available for all data sets. Both midrapidity densities and integrated yields are studied with the exception of the p-p collisions where the midrapidity data are not available. A compilation of p-p and heavy-ion data used in our analysis is summarized in Tables I and II.

The system-size dependence of ratios of particle yields is illustrated in Fig. 2 for the  $K^-/\pi^-$  and  $\bar{\Lambda}/\Lambda$ . The  $K^-/\pi^-$  ratio shows rather moderate dependence on the system size. The midrapidity data on the  $K^-/\pi^-$  ratio are almost saturated at the value expected for central Pb-Pb collisions already for  $N_{\text{part}} > 20$ , whereas the rapidity-integrated ratio shows such a property only for  $N_{\text{part}} > 30$ . The variation of the  $\bar{\Lambda}/\Lambda$  ratio with the system size is stronger than that observed in the  $K^-/\pi^-$  ratio. At mid-rapidity the  $\bar{\Lambda}/\Lambda$  ratio exceeds its value in the full phase-space by almost a factor of two.

The yield of  $\phi$ -mesons per pion in different colliding systems, normalized to its value in the most central Pb-Pb collisions, is shown in Fig. 3. The yield of  $\phi$ -mesons is seen to decrease stronger with decreasing system size than the pion yields. This indicates that the  $\phi$  with hidden strangeness does not behave like a strangeness-neutral object. For comparison, also shown in Fig. 3, are the results for the system-size dependence of the normalized  $K/\pi$  and  $(K/\pi)^2$  ratios. From the comparison with kaons its is not clear whether the  $\phi/\pi$  ratio favors the

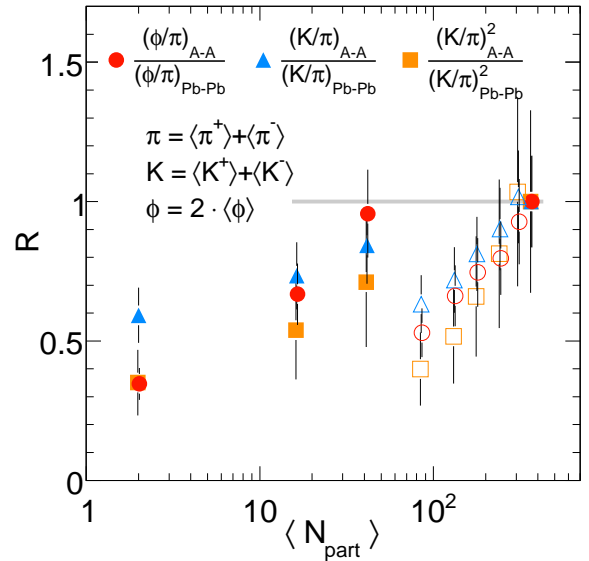


FIG. 3: The  $K/\pi$ ,  $(K/\pi)^2$  and  $\phi/\pi$  ratios of  $4\pi$  integrated yields normalized to their values in the central Pb-Pb collisions at the SPS. The p-p and central C-C, Si-Si and Pb-Pb data are from NA49 Collaboration at  $\sqrt{s_{NN}} = 17.3$  AGeV [16, 17, 18, 21, 22, 23, 24]. The open symbols refer to non-central Pb-Pb collisions.

single- or double-strange particle properties. Instead, it seems to behave as a strange particle with an effective quantum number between one and two.

### IV. MODEL COMPARISON WITH DATA

In the SM the particle production yields are fully determined by the thermal conditions in the collision fireball. In all models (a), (b) and (c) there is a common set of parameters  $(T, \mu_B, V)$  that quantifies the thermal particle yields. In the SM models (b) and (c), that account for an additional strangeness suppression, there are additional free parameters:  $\gamma_S$  and  $R_C$ , respectively. For our study, we used the code THERMUS [25].

Before considering a detailed quantitative analysis of particle production for different systems within the SM we first discuss general trends expected within the models based on the data shown in Figs. 2 and 3.

#### A. General trends

In terms of the models (a), (b) and (c) the anti-strange to strange particle ratios are independent of the fireball volume. In the C ensemble an explicit dependence of  $n_s$  on the volume appears in the same way for particles and anti-particles, thus it is cancelled in their ratios. Consequently, the strong variation of the  $\bar{\Lambda}/\Lambda$  ratio with the system size seen in Fig. 2 could be related to the variation in  $T$  and/or  $\mu_B$  with the system size. It

TABLE II:  $4\pi$ -integrated particle yields (upper part) and midrapidity densities (lower part) in central C-C, Si-Si and Pb-Pb collisions at  $\sqrt{s_{NN}} = 17.3$  GeV and fit results from model (c). The experimental results were taken from Ref. [16, 21] for C-C and Si-Si and from Ref. [19, 22] for Pb-Pb.

Particle	C-C		Si-Si		Pb-Pb	
	Data	Fit	Data	Fit	Data	Fit
$\pi^+/\pi^-$	$1.01 \pm 0.12$	1.01	$0.98 \pm 0.11$	0.98	$0.97 \pm 0.10$	0.99
$K^+/K^-$	$1.70 \pm 0.30$	1.71	$1.68 \pm 0.26$	1.70	$1.98 \pm 0.27$	1.77
$\bar{\Lambda}/\Lambda$	$0.134 \pm 0.039$	0.134	$0.127 \pm 0.033$	0.127	$0.083 \pm 0.023$	0.080
$K^-/\pi^-$	$0.067 \pm 0.011$	0.067	$0.077 \pm 0.010$	0.077	$0.081 \pm 0.010$	0.082
$\Lambda/K^+$	$0.52 \pm 0.18$	0.52	$0.52 \pm 0.13$	0.51	$0.44 \pm 0.10$	0.51
$\bar{\Lambda}/K^-$	$0.119 \pm 0.031$	0.119	$0.111 \pm 0.036$	0.111	$0.072 \pm 0.015$	0.072
$\pi^-$	$22.2 \pm 1.9$	22.2	$57.6 \pm 4.6$	57.6	$639 \pm 48$	639
$\pi^+/\pi^-$	$0.98 \pm 0.21$	1.07	$0.99 \pm 0.19$	1.03	$0.97 \pm 0.08$	0.99
$K^+/K^-$	$1.60 \pm 0.28$	1.30	$1.60 \pm 0.26$	1.46	$1.76 \pm 0.15$	1.62
$\bar{\Lambda}/\Lambda$	$0.269 \pm 0.085$	0.276	$0.182 \pm 0.070$	0.179	$0.140 \pm 0.044$	0.122
$K^-/\pi^-$	$0.093 \pm 0.018$	0.094	$0.100 \pm 0.018$	0.101	$0.096 \pm 0.008$	0.097
$\Lambda/K^+$	$0.280 \pm 0.063$	0.312	$0.366 \pm 0.081$	0.396	$0.361 \pm 0.082$	0.459
$\bar{\Lambda}/K^-$	$0.121 \pm 0.034$	0.112	$0.107 \pm 0.037$	0.104	$0.089 \pm 0.022$	0.091
$\pi^-$	$5.70 \pm 0.85$	5.70	$15.0 \pm 2.0$	15.0	$175.4 \pm 9.7$	175.4

is quite natural to assume that the temperature reached in the collision scales approximately with the collision energy. Therefore, at fixed  $\sqrt{s_{NN}}$  the temperature is expected to show a weak variation with the system size. On the other hand, the chemical potential can be viewed as the measure of baryonic stopping in the collision. Thus it should decrease with  $\sqrt{s_{NN}}$  and increase with system size. With the above generic properties of thermal parameters, the strong variation of  $\bar{\Lambda}/\Lambda$  with the system size seen in Fig. 2 could be attributed to a change in  $\mu_B$  at  $T \simeq const.$ , since in the SM  $\bar{\Lambda}/\Lambda \sim \exp(-2\mu_B/T)$ .

In the SM the  $K^-$  yield is not explicitly dependent on  $\mu_B$ . However, due to strangeness neutrality,  $\mu_S = \mu_S(\mu_B)$ , implying a weak influence of  $\mu_B$  on the kaon yield. Consequently, the change in the  $K/\pi$  ratio with the system size is mainly to be expected as a consequence of canonical suppression and/or chemical off-equilibrium effects.

In the equilibrium statistical models (a) and (c) the  $\phi$ -meson, being a strangeness neutral particle, should show similar system-size dependence as any other non-strange meson. Thus, the strong variation of the  $\phi/\pi$  ratio with centrality seen in Fig. 3 is inconsistent with the SM (a) and (c). The system-size dependence of  $\phi$ -mesons is only expected to be qualitatively different from the other mesons in the model (b) that accounts for strangeness suppression by including chemical off-equilibrium parameter  $\gamma_S$ . In this model the  $\phi$ -meson, being made of a strange/antistrange quark pair, is suppressed by the factor  $\gamma_S^2$ , thus behaving as a strangeness-two particle. However, from the discussion in the last section it is clear that, on the basis of data, it is not possible to fix the effective strangeness content of the  $\phi$ -meson. Consequently, to avoid ambiguities, we have excluded the hidden-strange

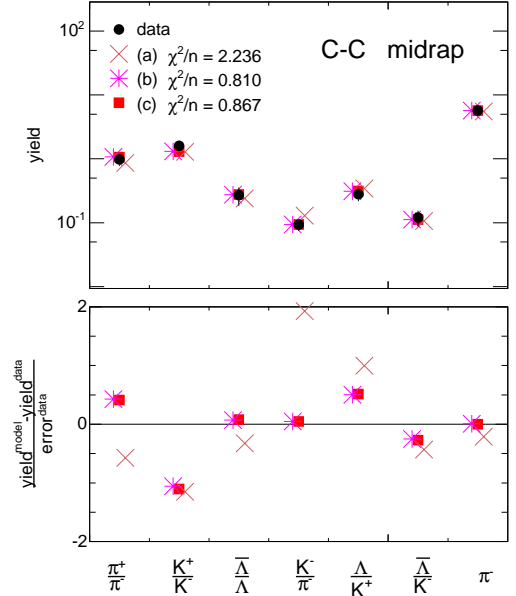


FIG. 4: Midrapidity  $\pi^-$ -density and midrapidity particle ratios from C-C collisions at  $\sqrt{s_{NN}} = 17.3$  AGeV from NA49 [16, 21] together with different model predictions: (a), (b) and (c) introduced in the text. The lower panel shows the  $\chi^2$ -deviations of the model fits to data.

particles from the SM analysis.

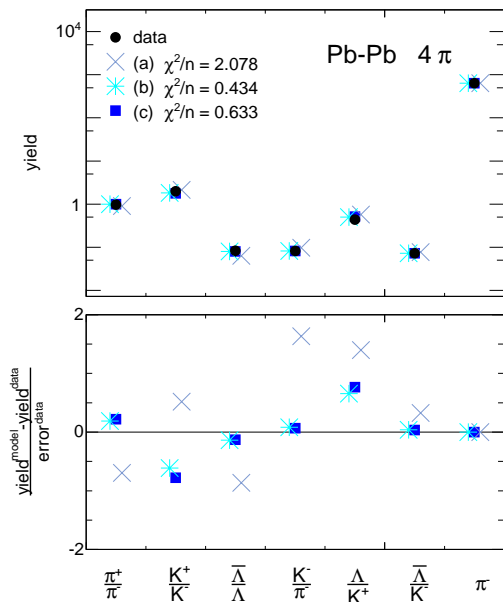


FIG. 5: Integrated  $\pi^-$  yield and integrated particle ratios from Pb-Pb collisions at  $\sqrt{s_{NN}} = 17.3$  AGeV [19, 22] together with the model fits as in Fig. 4. The lower panel shows the deviation of the model fits to data.

### B. System-size dependence of thermal parameters

The bulk properties of the system-size dependence of different particle yields in A-A collisions at the top SPS energy show qualitative agreement, except for the  $\phi$ -meson yields, with the expectations of the statistical models. To verify the validity of the models requires detailed quantitative studies. In the following, we analyze the SPS data from p-p, C-C, Si-Si and Pb-Pb collisions in terms of three different concepts that were introduced as: (a), (b) and (c) in the previous section. The investigated yields and ratios (listed in Tables I and II) together with model predictions are shown in Figs. 4 and 5 for C-C and Pb-Pb collisions respectively. Particle ratios from the fits with the best  $\chi^2$  are displayed for all of the models. The model (a) with a completely equilibrated strangeness abundance exhibits large deviations from data. The normalized differences between the model results and the data are shown in the lower panels of these figures. For the small systems, model (a) features very large values of  $\chi^2 \sim 2$  per degree of freedom. Thus, the equilibrium SM with strangeness conservation in the C ensemble is not favored by the data. In contrast, both models that allow for an extra suppression of the strange-particle phase-space with  $\gamma_S$  or with  $R_C$ , agree quite well with the measurements and yield comparably good descriptions of data. The latter can be correlated to properties of the hot and dense medium and systematic studies might provide access to the production and hadronization mechanism of strange particles.

The system-size dependence of thermal parameters ob-

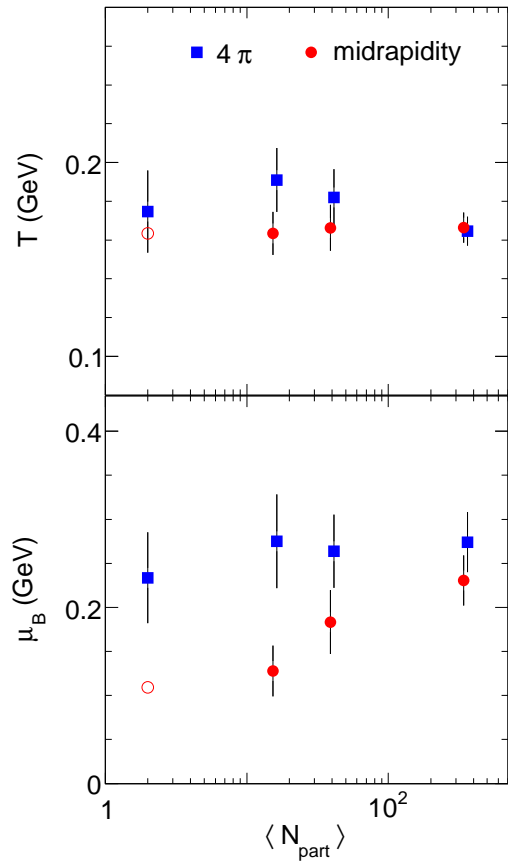


FIG. 6: Chemical freeze-out temperature  $T$  and baryon chemical potential  $\mu_B$  from fits to midrapidity densities (circles) and integrated yields (squares) from p-p and central C-C, Si-Si and Pb-Pb collisions obtained in the canonical model (c) introduced in the text. The open circles refer to the baryon chemical potential at midrapidity extracted from the  $\bar{\Lambda}/\Lambda$  ratio keeping  $T$  as for C-C collisions.

tained in these studies within the models (a) and (b) agree with previously published results and thus will not be discussed here. Instead, in Figs. 6, 7 and 8 we concentrate on the system-size dependence of thermal parameters characterizing the canonical model (c) with cluster formation. The corresponding values are summarized in Table III.

The freeze-out temperature  $T$  extracted from midrapidity data is barely dependent on the system size, as shown in Fig. 6. This is in agreement with the expectation that the chemical freeze-out temperature is predominantly established by the collision energy. Within statistical errors the  $4\pi$  data are also consistent with having the same chemical freeze-out temperature for all colliding systems from p-p up to Pb-Pb.

No significant change in the baryon chemical potential is seen in Fig. 6 for  $4\pi$  data. The variation of  $\bar{\Lambda}/\Lambda$  seen in the  $4\pi$  data in Fig. 2 is a combined effect of minor



TABLE III: Statistical model parameters, extracted from the comparison of model (c) with experimental data from full phase-space ( $4\pi$  integrated) (upper part) and midrapidity densities (lower part) in minimum bias p-p, central C-C, Si-Si and Pb-Pb collisions at  $\sqrt{s_{NN}} = 17.3$  GeV.

Reaction	$T(\text{MeV})$	$\mu_B(\text{MeV})$	$R(\text{fm})$	$R_C(\text{fm})$
p-p	$174.7 \pm 21.2$	$234 \pm 51$	$1.31 \pm 0.39$	$0.83 \pm 0.38$
C-C	$191.0 \pm 16.5$	$275 \pm 53$	$2.09 \pm 0.49$	$0.74 \pm 0.20$
Si-Si	$181.9 \pm 14.6$	$264 \pm 42$	$3.19 \pm 0.63$	$0.92 \pm 0.20$
Pb-Pb	$164.6 \pm 7.5$	$274 \pm 34$	$8.9 \pm 1.1$	$1.26 \pm 0.19$
C-C	$163.4 \pm 11.1$	$128 \pm 29$	$1.99 \pm 0.32$	$1.22 \pm 0.30$
Si-Si	$166.3 \pm 11.8$	$183 \pm 36$	$2.58 \pm 0.46$	$1.29 \pm 0.33$
Pb-Pb	$166.4 \pm 7.8$	$231 \pm 28$	$5.71 \pm 0.67$	$1.32 \pm 0.20$

changes in the freeze-out temperature and the chemical potential in different systems. At midrapidity, the chemical potential shows a decrease by almost 100 MeV from central Pb-Pb to C-C collisions at constant temperature. Consequently, there is a steep increase of the  $\bar{\Lambda}/\Lambda$  ratio, as seen in Fig. 2.

From the above results it is clear that at  $y = 0$  the collision fireball created in A-A collisions appears at constant temperature but with varying  $\mu_B$  that decreases with decreasing  $N_{\text{part}}$ . For the rapidity integrated data such systematics cannot be concluded.

In the canonical model (c) there are two volume scales that characterize the system: the fireball radius at freeze-out  $R$  and the strangeness correlation radius  $R_C$ . The fireball radius  $R$  is determined by the particle multiplicity e.g. the pion yield. Thus, a smaller pion density at midrapidity causes a smaller freeze-out radius than for the integrated yields.

The strangeness correlation volume  $R_C$  is extracted from the system-size dependence of the strange to non-strange particle ratios. The resulting system-size dependence of  $R_C$  is shown in Fig. 7. An increase of single-strange to non-strange particle ratios from p-p to Pb-Pb reactions is reflected in a variation of the strangeness correlation volume with the system size. The cluster radius varies between 0.7 fm and 1.3 fm. A larger radius in the fits of midrapidity data is correlated with the experimental observation of larger  $K^+/\pi^+$  ratios at midrapidity as compared to  $4\pi$  yields.

## V. DISCUSSION

We have already discussed in Fig. 1 that for strangeness-one particles the canonical suppression for  $R > (2 - 3)$  fm shows a very flat change with  $R$  and is hardly distinguishable from the asymptotic GC-value. Consequently, an exact determination of  $R_C$  based only on single-strange particles is very difficult and requires high precision data. For  $R > 3$  fm an increase of  $R_C$  by a large factor will not influence the particle yields significantly. Therefore, the results shown in Figs. 7 and 8 for  $N_{\text{part}} > 30$  or  $R > 5$  fm should be considered as a

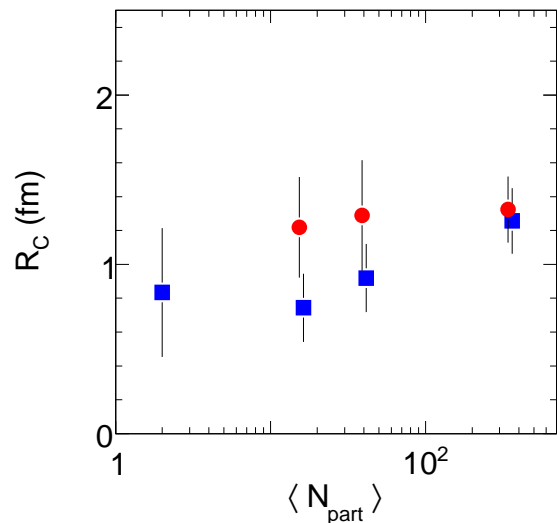


FIG. 7: Cluster radius  $R_C$  as a function of the system size in A-A collisions from fits of the model (c) to midrapidity densities (circles) and integrated yields (squares) from p-p and central C-C, Si-Si and Pb-Pb collisions.

lower limit. The actual change of  $R_C$  with system size and the chemical freeze-out radius could be stronger than that shown in Figs. 7 and 8. This happens, for example, at the SIS energy where the correlation volume  $V_C$  was shown to scale with the number of projectile participants [3]. A more precise determination of the relation between the volume at chemical freeze-out, system size and strangeness correlation at the SPS would require the analysis of the system size and/or centrality dependence of multi-strange particles in A-A collisions that show a stronger sensitivity to the strangeness correlation volume [14, 26, 27].

Relating the cluster to the fireball radii  $R_C = R_C(R)$ , it becomes clear that  $R_C$  has a significantly weaker system-size dependence than  $R$ , as seen in Fig. 8. In p-p collisions the strangeness correlation length  $R_C$  is almost as large as the fireball radius. In contrast, with increasing system size, the cluster volume can be even

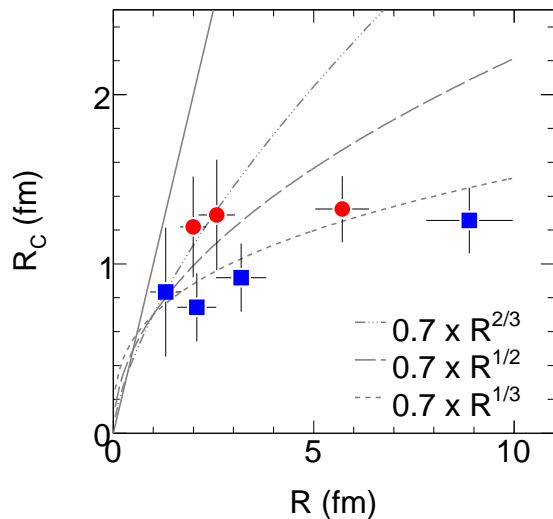


FIG. 8: Cluster radius  $R_C$  as a function of the fireball radius  $R$  from fits of the model (c) to midrapidity densities (circles) and integrated yields (squares) from p-p and central C-C, Si-Si and Pb-Pb collisions. The broken lines show various choices of the  $R_C = c R^\alpha$  relation. The full line indicates the proportionality  $R_C = R$ .

a few times smaller than the entire fireball. The dependence of  $R_C$  on  $R$  shown in Fig. 8 can be parameterized as  $R_C = c \cdot R^\alpha$  with  $\alpha < 1$  and  $c \simeq 0.7$  fm. From the consistent data set used in these studies the value of  $\alpha$  appears in the range  $1/3 < \alpha < 1/2$ . From this analysis we could conclude that the transition from suppressed (in p-p) to almost saturated (in Pb-Pb) single-strange particle production happens in a narrow range of the correlation length. This could indicate that  $R_C \simeq (1-2)$  fm is the

length scale of strangeness correlation. This suggestion gets implicit support from the percolation model calculations [28].

The appearance of a particle correlation volume in p-p collisions, introduced here for strangeness, comes also from other observables. The mass shift of the  $\rho^0$ -meson in the  $\pi^+\pi^-$  decay channel observed in p-p collisions [29] could not be substantially accounted for by the phase-space distortion of a Breit-Wigner line shape. It was argued [30] that re-scattering and re-interaction of pions contribute an additional term to the  $\rho^0$  spectral function. The best agreement with the measurement is achieved if a range of  $\pi^+\pi^-$  scattering of 0.73 fm is chosen. This value is in agreement with the strangeness correlation length  $R_C$  obtained in this study from the statistical model analysis of p-p data at the SPS.

In summary, two modified versions of the canonical statistical model have been investigated. The experimentally observed strong suppression of the strange-particle phase-space is retraced to local strangeness conservation within small correlated clusters in the fireball. These sub-volumes, in consequence, cause strong canonical suppression and allow one to successfully reproduce the experimental data. Furthermore, the cluster size is found to be only weakly dependent on system size. In all data under study, it is of the order of 1 to 2 fm.

## Acknowledgments

K.R. and J.C. acknowledge a partial support of the DFG under grant GRK 881. K.R. also acknowledges the support of the Polish Ministry of National Education (MEN).

- 
- [1] P. Braun-Munzinger, K. Redlich and J. Stachel, *Quark-Gluon Plasma 3*, edited by R. C. Hwa and Xin-Nian Wang (World Scientific Publishing, 2003), nucl-th/0304013.
  - [2] A. Andronic, P. Braun-Munzinger and J. Stachel, Nucl. Phys. A **772**, 167 (2006) [arXiv:nucl-th/0511071].
  - [3] J. Cleymans, H. Oeschler, K. Redlich, Phys. Rev. C **59** 1663 (1999).
  - [4] R. Hagedorn and K. Redlich, Z. Phys. C **27**, 541 (1985).
  - [5] F. Becattini, Z. Phys. C **69** (1995) 485.
  - [6] F. Becattini and U. Heinz, Z. Phys. C **76** (1997) 269.
  - [7] J. S. Hamieh, K. Redlich and A. Tounsi, Phys. Lett. B **486** (2000) 61.
  - [8] P. Braun-Munzinger, J. Cleymans, H. Oeschler, K. Redlich, Nucl. Phys. A **697** (2002) 902.
  - [9] F. Becattini, J. Manninen and M. Gazdzicki, Phys. Rev. C **73**, 044905 (2006); F. Becattini, J. Cleymans, A. Keranen, E. Suhonen and K. Redlich, Phys. Rev. C **64**, 024901 (2001).
  - [10] J. Rafelski and A. Tounsi, Phys. Lett. B **292** (1992) 417;
  - J. Letessier, J. Rafelski, A. Tounsi, Phys. Rev. C **50**, 406 (1994); C. Slotta, J. Sollfrank, U. Heinz, Proc. of Strangeness in Hadronic Matter (Tucson), (Ed. J. Rafelski), AIP conference proc. **340** (1995) p. 462.
  - [11] J. Cleymans, B. Kämpfer, S. Wheaton, Phys. Rev. C **65** (2002) 027901.
  - [12] J. Cleymans, B. Kämpfer, P. Steinberg, S. Wheaton, J. Phys. G **30** (2004) S595.
  - [13] A. Tounsi, A. Mischke, K. Redlich, Nucl. Phys. A **715** (2003) 565.
  - [14] H. Caines, J. Phys. G **32** (2006) S171.
  - [15] C. Höhne, F. Pühlhofer, R. Stock, Phys. Lett. B **640** (2006) 96.
  - [16] I. Kraus (NA49 Collaboration), J. Phys. G **31** S147 (2005), [nucl-ex/0412050].
  - [17] A. M. Rossi et al., Nucl. Phys. B **84** 269 (1975).
  - [18] S. V. Afanasiev et al. (NA49 Collaboration), Phys. Lett. B **491** 59 (2000).
  - [19] T. Anticic et al. (NA49 Collaboration), Phys. Rev. Lett. **93** 022302 (2004), [nucl-ex/0311024].



- [20] D. Barna (NA49 Collaboration), Ph.D. Thesis, University and KFKI Budapest, Hungary (2002).
- [21] C. Alt et al. (NA49 Collaboration), Phys. Rev. Lett. **94** 052301 (2005), [nucl-ex/0406031].
- [22] S. V. Afanasiev et al. (NA49 Collaboration), Phys. Rev. C **66** 054902 (2002).
- [23] F. Sikler (NA49 Collaboration), Nucl. Phys. A **661** 45c (1999).
- [24] V. Friese (NA49 Collaboration), Nucl. Phys. A **698** 487c (2002).
- [25] S. Wheaton and J. Cleymans, J. Phys. G31 (2005) S1069.
- [26] R. Stock, Phys. Lett. B **456** (1999) 277.
- [27] A. Tounsi and K. Redlich, J. Phys. G **28** S2095 (2002).
- [28] M. Nardi and H. Satz, Phys. Lett. B **442** 14 (1998).
- [29] J. Adams et al. (STAR Collaboration), Phys. Rev. Lett. **92** 092301 (2004).
- [30] P. Fachini, R. S. Longacre, Z. Xu and H. Zhang, J. Phys. G **33** (2007) 431.